

ACCEPTED VERSION

J. Deuerlein, S. Elhay, and A. R. Simpson

A fast graph matrix partitioning algorithm for solving the water distribution system equations

Journal of Water Resources Planning and Management, 2015; OnlinePubl:04015037-1-04015037-11

© 2015 American Society of Civil Engineers.

[10.1061/\(ASCE\)WR.1943-5452.0000561](https://doi.org/10.1061/(ASCE)WR.1943-5452.0000561)

PERMISSIONS

<http://dx.doi.org/10.1061/9780784479018.ch03>

p. 12 – Posting papers on the Internet

Authors may post the final draft of their work on open, unrestricted Internet sites or deposit it in an institutional repository when the draft contains a link to the bibliographic record of the published version in the ASCE Civil Engineering Database. “Final draft” means the version submitted to ASCE after peer review and prior to copyediting or other ASCE production activities; it does not include the copyedited version, the page proof, or a PDF of the published version.

8 July, 2015

<http://hdl.handle.net/2440/92996>

A fast graph matrix partitioning algorithm for solving the water distribution system equations

by

Deuerlein, J., Elhay, S. and Simpson, A. R.

Journal of Water Resources Planning and Management

Citation:

Deuerlein, J., Elhay, S. and Simpson, A. R. (2015). "A fast graph matrix partitioning algorithm for solving the water distribution system equations." *Journal of Water Resources Planning and Management*, Accepted April. (corresponding author: Jochen Deuerlein)

For further information about this paper please email Angus Simpson at angus.simpson@adelaide.edu.au

1
2
3
4
5
6
7
8
9
10
11
12
13
14
15
16
17
18
19
20
21
22
23
24
25
26
27

A Fast Graph Matrix Partitioning Algorithm for Solving the Water Distribution System Equations

J. Deuerlein^{1,3}, S. Elhay² and A. R. Simpson³, M.ASCE

Abstract:

In this paper a method which determines the steady-state hydraulics of a water distribution system, the Graph Matrix Partitioning Algorithm (GMPA), is presented. This method extends the technique of separating the linear and nonlinear parts of the problem and using the more time consuming nonlinear solver only on the nonlinear parts of the problem and faster linear techniques on the linear parts of the problem. The previously developed Forest-Core Partitioning Algorithm (FCPA) used this approach to separate the network graph's external forest from its looped core but did not address the fact that within the core of a network graph there may be many internal trees - nodes in series - for which a more economical linear process can be used. This extension of the separation process can significantly reduce the dimension of the nonlinear problem that must be solved: GMPA applied to eight case study networks with between 900 and 20,000 pipes show reductions to between 5% and 55% of the core dimension (after FCPA). The separation of the problem into its nonlinear and linear parts involves no approximations, such as lumping or skeletonization, and the resulting solution is precisely the solution that would have been obtained by the slower technique of solving the entire network with a nonlinear solver. The new method is applied after the network has been separated into an external forest and core by the FCPA method. The GMPA identifies all the nodes in the core which are in series (the internal forest) and then iterates alternately on the remaining core (the (nonlinear) global step) and the internal forest (the (linear) local step). In this paper, it is formally shown that the smaller set of nonlinear equations in the GMPA corresponds to the network equations of a particular topological subgraph of the original graph. Using algebraic manipulations, the size of the linearized system to be solved is reduced to the number of nodes in the core having degree greater than two. For pipe models of real world applications that are derived from GIS datasets, this can mean a dramatic reduction of the size of the nonlinear problem that has to be solved. The main contributions of the paper are (i) the

28 derivation and presentation of formal proofs for the new method and (ii) demonstrating how
29 significant the reduction in the dimension of the nonlinear problem can be for suitable networks. The
30 method is illustrated on a simple example.

31 **Keywords: Water Distribution Systems, Hydraulic Network Simulation, Graph Matrix**
32 **Decomposition, Forest-Core Partitioning**

33 ¹Senior Researcher and Partner, 3S Consult GmbH, Karlsruhe, Germany and Adjunct Senior Lecturer,
34 School of Civil, Environmental and Mining Engineering, University of Adelaide, Adelaide SA 5005,
35 Australia,
36 deuerlein@3sconsult.de

37 ²Visiting Research Fellow, School of Computer Science, University of Adelaide, South Australia,
38 5005, sylvan.elhay@adelaide.edu.au.

39 ³Professor, School of Civil, Environmental and Mining Engineering, University of Adelaide, Adelaide
40 SA 5005, Australia, angus.simpson@adelaide.edu.au.

41 **INTRODUCTION**

42 The calculation of steady-state hydraulic solutions of networks of elements has a long history. Early
43 on in 1936, Cross presented a method for the iterative solution of the linear mass balance and
44 nonlinear equations representing conservation of energy. Later, different methods for the simultaneous
45 solution of the equations were proposed by Epp and Fowler (1970). In this context, the relation to
46 graph theory was also established (Kesavan and Chandrashekar 1972, Gupta and Prasad 2000). The
47 most prevalent methods are the nodal method, the loop flow correction method (e.g. Nielsen 1989) and
48 the Global Gradient Algorithm (GGA) (Todini and Pilati 1988). The equivalent formulation of the
49 steady-state equations as a minimization problem that is derived from a variational principle has the
50 advantage that both the existence and uniqueness of solutions can be proven and powerful techniques
51 of convex optimization can be applied to the problem (Birkhoff and Diaz 1956, Birkhoff 1963,
52 Carpentier and Cohen 1993, Cherry 1951, Collins et al. 1978), even in the case where feedback
53 devices have to be considered in addition to pipes, valves and pumps (Deuerlein et al. 2009). An
54 overview of existing methods has been published recently (Todini and Rossman 2013).

55 Although remarkable speed increases have been achieved by hydraulic solvers, optimization
56 algorithms, in particular evolutionary algorithms that require a huge number of repeated network
57 solution calculations in which the network topology does not change still suffer from long computing
58 times. In addition, speed of computation is important when algorithms are used online for real-time
59 analysis. As a result, a speed-up of existing hydraulic simulation methods is required.

60 One application of hydraulic online simulation relates to water network security. Online simulation is
61 used for monitoring of the current state of the network. As well, in the case of a contamination event,
62 additional functions such as source identification and development of mitigation measures are based
63 on the knowledge of the actual hydraulic state of the system. These functions again require the
64 simulation of a number of different scenarios with various levels of detail. Reducing the size of the
65 most time-consuming nonlinear problem will help.

66 Various commercial and non-commercial software programs are available for calculating the hydraulic
67 steady-state condition of a network. Many of them are based on the Global Gradient Algorithm
68 (Todini and Pilati 1988), which, for instance, is implemented in EPANET (Rossman 2000). In this
69 paper, a graph matrix partitioning method is presented that solves the global set of equations but
70 significantly reduces the size of the linearized system of equations that is solved in each iteration. The
71 method is based on a decomposition concept of the network graph (Deuerlein 2008). In that
72 publication it was shown that, in demand-driven analysis, the hydraulic steady-state equations of the
73 forest can be solved independently from the core. The concept of forest-core partitioning was further
74 developed by Simpson et al. (2014). The core can be further subdivided into bridge components and
75 looped blocks. A non-linear solver is required only for the blocks. The content of this manuscript
76 addresses a faster solution method for the significantly smaller set of the non-linear block equations
77 that is based on the partitioning of the nodes of the blocks into supernodes (degree > 2) and internal
78 nodes (degree = 2).

79

80 The GMPA begins by using the FCPA to separate the network core from the external forest (the forest
81 which consists of all the trees which have leaf nodes (nodes with index 1)) and then identifying, within

82 the core, all those nodes which have index 2 (the internal forest). The GMPA exploits the fact that the
83 solution for the internal forest can, like the external forest) be achieved by a much faster linear solver.
84 As a result, only the smaller part of the core (which remains when the internal trees have been
85 partitioned for separate treatment), needs a nonlinear solver.

86

87 Giustolisi et al. (2010, 2012) presented the Enhanced Global Gradient Algorithm (EGGA), which uses
88 heuristically based transformation matrices to exploit the presence of nodes with index 2. However, (i)
89 GMPA includes a preliminary forest-core partitioning step (Simpson et al. 2014), (ii) allows the
90 inclusion of control devices by appropriate selection of internal tree chords, (iii) and is presented with
91 a formal derivation and rigorous proof of the method.

92

93 One possible approach for reducing calculation time is the aggregation of existing models that are
94 usually derived from comprehensive Geographical Information Systems (GIS) datasets. In this case, a
95 similar simplified system is created by merging of links of the same diameter and eliminating the
96 nodes connecting these links. However, the resulting model is only an approximation of the original
97 system and the connection to the original reference data taken from a GIS may be lost.

98

99 The structure of the paper is as follows: After a brief review of the fundamental equations, some basics
100 on the subgraph concept are presented. In the main part of this paper, the equivalence of the GMPA
101 that is based on the topological subgraph to the full set of equations is stated. A proof is then given. It
102 is shown that the new method subdivides the solution procedure into global and local steps. In the
103 global step, a nonlinear system of equations has to be solved for the topological subgraph. The
104 solution of the local step consists of linear algebraic calculations applying the global solution to
105 determine the flows and heads of the internal trees. An example system is used to illustrate the
106 method. Eight case-study networks, with between 900 and 20,000 pipes, and which were considered in
107 Simpson et al (2014), are used to illustrate the significant reduction achieved by GMPA in the size of
108 the nonlinear problem that must be solved.

109

110 BACKGROUND

111 Mathematical Modeling of Water Distribution Systems

112 As mentioned in an earlier paper (Deuerlein et al., 2009), an alternative formulation to solving the pipe
113 network equations by direct methods may be based on the minimization methods of nonlinear
114 optimization. Birkhoff and Diaz (1956) and later Birkhoff (1963) have shown that the calculation of
115 the looped electrical circuit systems with consideration of the first and second laws of Kirchhoff is
116 equivalent to the minimization of a convex function. These principles also can be applied to solving
117 the pipe network equations, which are modelled by analogous equations. Using the work of Cherry
118 (1951) and Millar (1951) for the calculation of electrical networks, Collins et al.(1978) applied the
119 minimization of the Content and Co-Content functions to the calculation of the steady-state for
120 hydraulic networks. The problem of minimizing the Content function can be stated as follows:

$$121 \quad \begin{aligned} & \min_{\mathbf{q} \in \mathbb{R}^m} C(\mathbf{q}) \\ & s. t. \quad \mathbf{A}^T \mathbf{q} = -\mathbf{Q} \end{aligned} \quad (1)$$

122 Here, $C(\mathbf{q})$ denotes the system content, m is the number of pipes, $\mathbf{q} \in \mathbb{R}^m$ is the vector of pipe flows,
123 $\mathbf{A} \in \mathbb{R}^{m \times n}$ is the link-node incidence matrix of pipes and demand nodes (number n) with $A_{j,i} = 1$ if
124 node i is the final node of link j , $A_{j,i} = -1$ if node i is the first node of link j and $A_{j,i} = 0$, otherwise.
125 $\mathbf{Q} \in \mathbb{R}^n$ is the vector of given nodal demands (for withdrawals $Q_i < 0$). The equality constraints
126 consist of the continuity equations of the demand nodes. The total system content is composed of the
127 sum of the single contents of the network elements. The content of pipe j is given by

$$128 \quad C_j = \int_0^{q_j} \left(r_j |x_j|^{\alpha-1} + K_j |x_j| \right) x_j dx_j. \quad (2)$$

129 Here, q_j is the flow for pipe j , $r_j = r_j(x_j)$ is the pipe resistance which depends on flow for the Darcy-
130 Weisbach head loss and α the exponent of the hydraulic equation (usually for the Darcy-Weisbach or
131 Hazen-Williams formulations where $\alpha \geq 1$). The second term refers to the local minor loss of valves
132 and fittings. If all the content functions are strictly convex (which is guaranteed by the strict
133 monotonicity of the head loss equation) and norm-coercive ($|C_j(q_j)| \rightarrow \infty$ if $\|q_j\| \rightarrow \infty$) then the
134 total system content is a strictly convex and norm-coercive function of \mathbf{q} . As a result, there exists a
135 unique solution if, in addition, the constraints are affine. The proof of existence is a very important

136 result and can be found for example in Piller (1995). In this case, the Lagrangian of Eq. (1) gives a
 137 necessary and sufficient condition for the solution:

$$138 \quad \begin{bmatrix} \mathbf{F} & \mathbf{A} \\ \mathbf{A}^T & \mathbf{0} \end{bmatrix} \begin{bmatrix} \mathbf{q} \\ \boldsymbol{\lambda} \end{bmatrix} = \begin{bmatrix} -\mathbf{A}_R \mathbf{H}_R \\ -\mathbf{Q} \end{bmatrix} \quad (3)$$

139 where $\mathbf{F} \in \mathbb{R}^{m \times m}$ is a diagonal matrix and the product of $\mathbf{F}\mathbf{q}$ are the link head losses. The elements of
 140 the diagonal matrix \mathbf{F}_k are defined by $F_{k,j,j} = r_j |q_{k,j}|^{\alpha-1} + K_j |q_{k,j}|$ where the first term refers to the
 141 head losses due to friction along the pipe wall and the second term includes local minor losses of
 142 valves and fittings (K_j : minor loss coefficient).

143 On the right hand side of Eq. (3) $\mathbf{A}_R \in \mathbb{R}^{m \times nr}$ and $\mathbf{H}_R \in \mathbb{R}^{nr}$ refer to the incidence matrix of fixed
 144 head nodes and vector of fixed heads, respectively in Eq. (3), nr is the number of fixed head nodes.
 145 The Lagrange multipliers $\boldsymbol{\lambda} \in \mathbb{R}^n$ that correspond to the affine mass balance constraints or nodal flow
 146 continuity equations in Eq. (1) are actually the nodal heads at the demand nodes.

147 The solution to the non-linear system Eq. (3) is often found iteratively by Newton's method

$$148 \quad \begin{bmatrix} \mathbf{D}_k & \mathbf{A} \\ \mathbf{A}^T & \mathbf{0} \end{bmatrix} \begin{bmatrix} \mathbf{q}_{k+1} - \mathbf{q}_k \\ \mathbf{H}_{k+1} - \mathbf{H}_k \end{bmatrix} = - \begin{bmatrix} \mathbf{F}_k \mathbf{q}_k + \mathbf{A} \mathbf{H}_k + \mathbf{A}_R \mathbf{H}_R \\ \mathbf{A}^T \mathbf{q}_k + \mathbf{Q} \end{bmatrix}, \quad (4)$$

149 provided \mathbf{D}_k , which is the derivative of the head losses $\mathbf{F}\mathbf{q}$, is invertible. The vector $\mathbf{q}_{k+1} - \mathbf{q}_k$
 150 includes the unknown changes in link flows, $\mathbf{H}_{k+1} - \mathbf{H}_k$ is the vector of unknown nodal head changes,
 151 \mathbf{H}_R is the vector of known heads and \mathbf{Q} is the vector of known nodal demands or input flows.

152 The GGA of Todini and Pilati (1988), a two-stage implementation of Eq. (4), finds the unknown nodal
 153 heads, \mathbf{H}_{k+1} (Lagrangian multipliers $\boldsymbol{\lambda}$ in Eq. (3)) in one-step and then finds the pipe flows, \mathbf{q}_{k+1} , by a
 154 simple update process:

$$155 \quad \mathbf{A}^T \mathbf{D}_k^{-1} \mathbf{A} \cdot \mathbf{H}_{k+1} = \mathbf{Q} + \mathbf{A}^T \mathbf{q}_k - \mathbf{A}^T \mathbf{D}_k^{-1} \mathbf{F}_k \cdot \mathbf{q}_k - \mathbf{A}^T \mathbf{D}_k^{-1} \mathbf{A}_R \cdot \mathbf{H}_R$$

$$156 \quad \mathbf{q}_{k+1} = \mathbf{q}_k - \mathbf{D}_k^{-1} [\mathbf{F}_k \mathbf{q}_k + \mathbf{A} \mathbf{H}_{k+1} + \mathbf{A}_R \mathbf{H}_R] \quad (5)$$

157 The second part of Eq. (5) is solved simply because the matrix \mathbf{D}_k^{-1} is diagonal. The first part, which is
 158 more difficult to solve, includes the solution of a linear system of size n . In all iterations after the first,

159 the calculated flows will satisfy the continuity equations independently of the starting point (initial
160 flow vector) of the algorithm (see Elhay et al., 2014).

161 Recall that the size of \mathbf{D}_k is the total number of links in the graph of the full network. For constant r_j
162 the derivative matrix is $D_{k,j,j} = \alpha r_j |q_{k,j}|^{\alpha-1} + 2K_j |q_{k,j}|$ but in the case of the Darcy-Weisbach
163 formula, r_j is also a function of $q_{k,j}$ and the calculation of the derivative is more complicated (see
164 Simpson and Elhay 2011 for details).

165 **THE GRAPH MATRIX PARTITIONED ALGORITHM**

166 **Decomposition to form the reduced topological subgraph system**

167 The first step of the GMPA consists of the identification of the “forest” of the network graph. The
168 forest consists of trees that are connected to bridge components or looped blocks at their root node.
169 Figure 1 shows a simplified example network graph that has typical topological properties of a real
170 water supply system. Branched trees leading to the end-user demands are connected to a looped
171 distribution system at the root nodes. From graph theory, it is known that the incidence matrix of a tree
172 (without its root node) is square and invertible. Therefore, in demand driven analysis, the flows of the
173 forest pipes can be calculated (see Simpson et al. 2014 for details of calculation method) by using just
174 the (linear) continuity equations as a preliminary step before the iterative solution procedure is applied
175 to the “core” of the network.

176

177 In what follows it is assumed that the forest has already been virtually separated from the network
178 graph and the demand at the root node of each removed tree has been increased by the total demand of
179 the tree. The separation does not involve any approximation or lumping. At the end of the process, the
180 solution obtained is precisely the solution for the whole (original) network. The resulting graph $G_C \subseteq$
181 $G = (V, E)$ is called the “core” of the original network graph. It can be shown that G_C is an (induced)
182 subgraph of the original graph $G_C \subseteq G = (V, E)$. More details on the separation of the forest and core
183 decomposition can be found in the literature (Diestel 2010; Deuerlein 2008). From Figure 1, it can be
184 seen that the root nodes (filled with black) of all the trees have degree three or greater (degree: number
185 of connected links at node). After separating each of the trees, most of the root nodes have degree two

186 in the core graph (see Figure 2). This property is used for the next step where the core graph G_C is
187 further simplified by the identification of “supernodes” and “superlinks.”

188 Supernodes have the property that they connect at least three links of the original core graph (nodes E
189 and I in Figure 3). A superlink can be understood as virtual link that represents the series of links
190 between the two supernodes. The nodes inside the path that connects the supernodes are called
191 “internal tree nodes” (index I, nodes F, G and H in Figure 3). The series of links connecting the two
192 supernodes with the last link removed is called the internal tree (E - F - G -H), and finally, the link (H-
193 I) is called the internal co-tree chord. The reason for the terminology “internal tree” and “internal co-
194 tree chord will become clear later.

195 The (topological) subgraph $G_S = (V_S, E_S)$ consists of the vertex set of supernodes V_S with $|V_S| = n_S$
196 and the arc set of superlinks E_S with $|E_S| = m_S$. Note that G_S refers to the topological subgraph of the
197 core of the original network graph that results from link contractions that are iteratively applied to
198 links that have at least one node of degree 2 in the core subgraph. The resulting topological subgraph
199 is maximal in the sense that all the nodes with degree 2 are separated. The graph G_S is smaller than the
200 full core graph for the network if the network core has nodes in series. By means of graph theory it can
201 be shown that G_S is actually a topological minor of G and G_C : $G_S \preceq G_C \preceq G$. The minor relation \preceq is a
202 partial ordering of finite graphs, i. e. reflexive, antisymmetric and transitive (see Diestel 2010, p. 20).

203 In contrast, the full core graph G_C is called a subdivision of graph G_S . It follows that the two graphs G_S
204 and G_C are homeomorphic in the topological sense, which means that they have the same topological
205 properties; for instance, the number of loops remains the same for both G_C and G_S . Please note that the
206 term ‘topological’ used here refers to the fact, that in contrast to induced subgraphs, where the link set
207 of the subgraph is a subset of the original link set, here each superlink of the topological subgraph
208 replaced by a set of pipes in series each with internal vertices of degree 2. As a consequence, the links
209 of the original graph appear as superlinks in the subgraph only in the case where both end nodes have
210 degree > 2 in the original core graph.

211 **Hydraulic Steady-State Equations of the GMPA**

212 In this section, the GMPA method for demand driven hydraulic steady-state calculation of general
213 pressurized pipe systems which subdivides the solution process into a global step (for the graph G_S)

214 and a local step (for the internal trees) steps is presented. It will be shown that the dimension of the
215 system of equations that has to be solved during the iterations can be reduced to the number of
216 supernodes of the graph G_S that was introduced in the last section. For complex real-world water
217 supply systems, the size of the system to be solved can be reduced significantly for such systems. The
218 full derivation of the method from the basic network equations will be given in the next section. In this
219 context, the linear transformation mapping between full graph and topological subgraph will also be
220 discussed.

221 The global solution step is formulated as follows. The vertex set of G_S consists of a subset of n_S nodes
222 of the original graph, the supernodes. The set of links between supernodes of the original graph may
223 be treated as a set of m_S superlinks. Now assume that the heads of the supernodes are known (as
224 boundary conditions of the local subsystem) the series of pipes in-between can be understood as a
225 pseudo loop representing a subsystem that consists of two reservoirs that are connected by a series of
226 pipes. The heads and flows of these isolated subsystems can be efficiently calculated by the loop
227 method since the subsystem always consists of exactly one pseudo loop regardless of the number of
228 intermediate links in series. The superlink is the pseudo-link that represents the known pressure
229 difference between the supernodes and closes the pseudo-loop (see Figure 3). A well-known approach
230 for solving such a system is to separate the links of the loop into a spanning tree and a chord link.
231 Therefore, in the previous section, the term “internal tree” has been introduced for the internal
232 spanning tree that consists of “internal tree branches” and the term “internal tree chord” is used for the
233 link that is chosen arbitrarily as chord of the local pseudo-loop. The union of internal trees is called the
234 internal forest. Please note that in our case where the external forest has been separated by the FCPA
235 before the GMPA is applied and the method is applied to the network core, the internal tree is always a
236 path. However, the method can still be applied where the local systems have tree like structure (for
237 example if the trees of the global forest are not separated).

238

239 The superlinks in the GMPA have an important property: it is known (see Elhay et al., 2014) that the
240 continuity equations are satisfied after the first iteration of the GGA or the Reformulated Co-Tree
241 Flows Method (RCTM) (see Elhay et al., 2014) and so the flow corrections of all links that are

242 represented by a common superlink are identical. Thus, if the flow correction for one link (for example
 243 an internal co-tree chord belonging to the internal tree of the superlink) is known from the global step
 244 calculation, the other flows of the internal tree branches of that superlink can be calculated locally
 245 (local step). As mentioned before, in the global step a superlink replaces at least one link, the internal
 246 co-tree chord (index C), and the appropriate number of internal tree branches (index T). The total
 247 number of internal co-tree chords is equal to the number of superlinks and the number of internal tree
 248 branches is $m_T = m_{2core} - m_S$. The flows of the other internal tree branches are a linear function of
 249 the both flow of the last link and the given demands of the internal tree nodes. This is a very important
 250 feature of the GMPA and is the fundamental reason why a significant reduction in computation can be
 251 achieved. The system of equations of the global step (graph G_S) can be formulated in terms of the
 252 unknown superlink flows corrections, $[\mathbf{q}_{C,k+1} - \mathbf{q}_{C,k}]$, at iteration $k + 1$ and the heads corrections,
 253 $[\mathbf{H}_{S,k+1} - \mathbf{H}_{S,k}]$, at iteration $k + 1$:

$$254 \begin{bmatrix} \mathbf{D}_{S,k} & \mathbf{A}_S \\ \mathbf{A}_S^T & \mathbf{0} \end{bmatrix} \begin{bmatrix} \mathbf{q}_{C,k+1} - \mathbf{q}_{C,k} \\ \mathbf{H}_{S,k+1} - \mathbf{H}_{S,k} \end{bmatrix} = - \begin{bmatrix} \mathbf{h}_{S,k} + \mathbf{A}_S \mathbf{H}_{S,k} + \mathbf{A}_{S,R} \mathbf{H}_R \\ \mathbf{A}_S^T \mathbf{q}_{C,k} + \bar{\mathbf{Q}}_S \end{bmatrix} \quad (6)$$

255 with

$$256 \bar{\mathbf{Q}}_S = -\mathbf{A}_{S,T}^T (\mathbf{A}_{I,T}^T)^{-1} \mathbf{Q}_I + \mathbf{Q}_S \quad (6a)$$

$$257 \mathbf{h}_{S,k} = [\mathbf{F}_{C,k} + \mathbf{P} \mathbf{F}_{T,k} \mathbf{P}^T] \mathbf{q}_{C,k} - \mathbf{P} \mathbf{F}_{T,k} (\mathbf{A}_{I,T}^T)^{-1} \mathbf{Q}_I \quad (6b)$$

258 Eq. (6) forms the Newton iteration system for the topological subgraph G_S . The incidence matrix for
 259 the topological subgraph is $\mathbf{A}_S \in \mathbb{R}^{m_S \times n_S}$ and the diagonal matrix $\mathbf{D}_S \in \mathbb{R}^{m_S \times m_S}$ has the head loss
 260 derivatives of the superlinks. Submatrices $\mathbf{A}_{S,T} \in \mathbb{R}^{m_T \times n_S}$ and $\mathbf{A}_{I,T} \in \mathbb{R}^{m_T \times m_T}$ are blocks of the
 261 (permuted) original incidence matrix, $\mathbf{P} \in \mathbb{R}^{m_S \times m_T}$ is the incidence matrix for the internal forest of
 262 nodes with index 2 (the nodes which are in series). Matrices $\mathbf{Q}_I \in \mathbb{R}^{n_I}$ and $\mathbf{Q}_S \in \mathbb{R}^{n_S}$ are the blocks of
 263 the decomposed demand vector that refer to internal nodes (Index I) and supernodes (index S),
 264 respectively. Vector $\mathbf{q}_{C,k} \in \mathbb{R}^{m_S}$ includes the flows of internal co-tree chords according to Figure 3
 265 and $\mathbf{F}_{C,k} \in \mathbb{R}^{m_S \times m_S}$ and $\mathbf{F}_{T,k} \in \mathbb{R}^{m_T \times m_T}$ are two parts of the diagonal matrix \mathbf{F}_k of Eq. (5) that are
 266 decomposed into blocks for internal tree branches and internal co-tree chords. The matrices and the

267 objects which they model will be explained in more detail in the next section. In what follows we will
 268 denote $(\mathbf{A}_{I,T}^{-1})^T$ (which = $(\mathbf{A}_{I,T}^T)^{-1}$) by $\mathbf{A}_{I,T}^{-T}$.

269 The solution procedure here deals with a smaller set of equations than for the GGA if the core of the
 270 network has some nodes in series. The calculation of the head losses of the superlinks and the
 271 respective matrices $\mathbf{D}_{S,k}$ and $\mathbf{F}_{S,k}$ is carried out locally. Matrix $\mathbf{P} \in \mathbb{R}^{m_S \times m_T}$ represents the linear
 272 transformation between the links of G_C and G_S . Multiplication of a topological matrix on the left by \mathbf{P}
 273 collapses the branches of an internal tree onto a single superlink whereas right multiplication of a
 274 matrix by \mathbf{P} expands a superlink to the individual branches of the corresponding internal tree. The
 275 derivation of \mathbf{P} is given in the next section. Once the global unknowns $\mathbf{q}_{C,k+1}$ and $\mathbf{H}_{S,k+1}$ are known
 276 the local step of calculating the flows of internal tree branches and heads of internal tree nodes is
 277 straightforward. This results in two steps of the GMPA:

278 **The Global Step:** Calculation of heads of supernodes and flows of internal co-tree chords representing
 279 the superlinks

$$280 \quad \mathbf{A}_S^T \mathbf{D}_{S,k}^{-1} \mathbf{A}_S \mathbf{H}_{S,k+1} = \bar{\mathbf{Q}}_S + \mathbf{A}_S^T \mathbf{q}_{C,k} - \mathbf{A}_S^T \mathbf{D}_{S,k}^{-1} [\mathbf{h}_{S,k} + \mathbf{A}_{S,R} \mathbf{H}_R] \quad (7)$$

$$281 \quad \mathbf{q}_{C,k+1} = \mathbf{q}_{C,k} - \mathbf{D}_{S,k}^{-1} [\mathbf{h}_{S,k} + \mathbf{A}_S \mathbf{H}_{S,k+1} + \mathbf{A}_{S,R} \mathbf{H}_R] \quad (8)$$

282 **The Local Step:** Calculation of heads of the internal tree nodes and flows of the internal tree branches

$$283 \quad \mathbf{q}_{T,k+1} = \mathbf{P}^T \mathbf{q}_{C,k} - \mathbf{A}_{I,T}^{-T} \mathbf{Q}_I \quad (9)$$

$$284 \quad \mathbf{H}_{I,k+1} = -\mathbf{A}_{I,T}^{-1} [\mathbf{A}_{S,T} \mathbf{H}_{S,k+1} + \mathbf{A}_{R,T} \mathbf{H}_R + \mathbf{D}_{T,k} \mathbf{q}_{T,k+1}] \quad (10)$$

285 With the approach presented here, the number of unknowns of the linear system of equations that has
 286 to be solved at any iteration of the GMPA (Eq. (7)) is reduced to the number of supernodes n_S . Since
 287 $\mathbf{D}_{S,k}$ is a diagonal matrix, Eq. (8) consists of algebraic calculations. The same applies to the local step
 288 since matrix $\mathbf{A}_{I,T}$ has an analytical inverse, which will be shown later.

289
 290 **DERIVATION AND PROOF OF THE GRAPH MATRIX PARTITIONING ALGORITHM**

291 In what follows, the equivalence of the modified equations for the local and global steps (Eq. (7) to
 292 Eq. (10)) and the original GGA equations (Eq. **Error! Reference source not found.**) will be shown.

293 The basic idea is that the incidence matrix of the network graph can be partitioned into four blocks
294 where the upper right square block has full rank and is invertible.

295 **Partitioning of the Incidence Matrix**

296 In the new GMPA method, internal nodes are removed by an algebraic elimination process that is
297 applied to the full system of hydraulic network equations. It is important to note that the GMPA
298 method does not include any approximation. The elimination is based on permuting the rows and the
299 columns of the graph incidence matrix \mathbf{A} and the diagonal head loss derivative matrix \mathbf{D} of the original
300 system. Consider the partitioning of both the \mathbf{A} and \mathbf{D} matrices as follows:

$$301 \quad \mathbf{A} = \begin{bmatrix} \mathbf{A}_{S,T} & \mathbf{A}_{I,T} \\ \mathbf{A}_{S,C} & \mathbf{A}_{I,C} \end{bmatrix}, \quad \mathbf{D} = \begin{bmatrix} \mathbf{D}_T & \mathbf{0} \\ \mathbf{0} & \mathbf{D}_C \end{bmatrix} \quad (11)$$

302 where

303 **T:** Tree (branches of internal trees) (see #3 in Figure 3)

304 **C:** **Co-tree (Chords)** (chords of internal trees) (see #4 Figure 3)

305 **S:** Supernodes (E and I in Figure 3)

306 **I:** Internal nodes (F, G and H in Figure 3)

307 In what follows it will be assumed that the necessary permutations have already been performed: the
308 matrix \mathbf{A} is in the correct permuted form and \mathbf{D} is diagonal. It is shown in the Appendix A how to
309 permute \mathbf{A} in this way while preserving the diagonal structure of \mathbf{D} . The columns of \mathbf{A} refer to the
310 nodes of the graph G . The first column of the block matrix in Eq. (11) belongs to the supernodes (first
311 index S) and the second column belongs to internal tree nodes (first index I). In a similar way the
312 internal tree branches (second index T) are partitioned from the internal co-tree chords (second index
313 C) in matrices \mathbf{A} and \mathbf{D} . An important result of the reordering is that matrix $\mathbf{A}_{I,T}$ is always square and
314 invertible. Furthermore, it will be shown that its exact inverse can be computed quickly and simply.
315 This fact can be used for eliminating both the flows in the internal trees as well as the heads of the
316 internal tree nodes. The method can be understood as partitioning the solution process into one global
317 step (analysis of the network consisting of superlinks and supernodes only) and several local steps
318 (where the flows of the internal tree links are determined).

319

320 **System of equations**

321 Substitution of the matrices \mathbf{A} and \mathbf{D} from Eq. (11) into Eq. (5) results in the following system of
 322 linearized equations:

$$323 \begin{bmatrix} \mathbf{D}_{T,k} & \mathbf{0} & \mathbf{A}_{S,T} & \mathbf{A}_{I,T} \\ \mathbf{0} & \mathbf{D}_{C,k} & \mathbf{A}_{S,C} & \mathbf{A}_{I,C} \\ \mathbf{A}_{S,T}^T & \mathbf{A}_{S,C}^T & \mathbf{0} & \mathbf{0} \\ \mathbf{A}_{I,T}^T & \mathbf{A}_{I,C}^T & \mathbf{0} & \mathbf{0} \end{bmatrix} \begin{bmatrix} \mathbf{q}_{T,k+1} - \mathbf{q}_{T,k} \\ \mathbf{q}_{C,k+1} - \mathbf{q}_{C,k} \\ \mathbf{H}_{S,k+1} - \mathbf{H}_{S,k} \\ \mathbf{H}_{I,k+1} - \mathbf{H}_{I,k} \end{bmatrix} = \begin{bmatrix} d\mathbf{E}_T \\ d\mathbf{E}_C \\ d\mathbf{Q}_S \\ d\mathbf{Q}_I \end{bmatrix}_k \quad (12)$$

324 where

$$325 d\mathbf{E}_T = -(\mathbf{F}_{T,k} \mathbf{q}_{T,k} + \mathbf{A}_{S,T} \mathbf{H}_{S,k} + \mathbf{A}_{I,T} \mathbf{H}_{I,k} + \mathbf{A}_{R,T} \mathbf{H}_R),$$

$$326 d\mathbf{E}_C = -(\mathbf{F}_{C,k} \mathbf{q}_{C,k} + \mathbf{A}_{S,C} \mathbf{H}_{S,k} + \mathbf{A}_{I,C} \mathbf{H}_{I,k} + \mathbf{A}_{R,C} \mathbf{H}_R),$$

$$327 d\mathbf{Q}_S = -(\mathbf{A}_{S,T}^T \mathbf{q}_{T,k} + \mathbf{A}_{S,C}^T \mathbf{q}_{C,k} + \mathbf{Q}_S),$$

$$328 d\mathbf{Q}_I = -(\mathbf{A}_{I,T}^T \mathbf{q}_{I,k} + \mathbf{A}_{I,C}^T \mathbf{q}_{C,k} + \mathbf{Q}_I),$$

329 Further developments are based on the following:

330 **Lemma 1:**

331 a) Matrix $\mathbf{A}_{I,T}$ is square and invertible.

332 b) $\mathbf{A}_{I,T}$ is block diagonal with lower triangular diagonal blocks, all the elements of which are in $\{-$
 333 $1,0,1\}$, and has an exact inverse which is easily computed.

334 **Proof:**

335 a) Let m_S be the number of links (internal tree branches and an internal co-tree chord) represented by a
 336 superlink. Then, the number of nodes of the internal tree and internal co-tree is m_S+1 . If the last link
 337 (for example link HI in Figure 3) is separated then the resulting structure is an internal tree.

338 $\mathbf{A}_{I,T}$ includes for each superlink the series of internal links except for the last link. The resulting
 339 subgraph is always a tree (i.e. it is connected and has no loops). The nodes of $\mathbf{A}_{I,T}$ are the interior
 340 nodes. The root of the tree is the initial node of the superlink, which is not part of $\mathbf{A}_{I,T}$. It is well
 341 known from graph theory (Diestel 2010) that the incidence matrix of a tree without its root node is
 342 always square and invertible. It follows that the matrix $\mathbf{A}_{I,T}$ consisting of diagonal blocks of simple
 343 tree incidence matrices is always invertible (see solid links in Figure 3).

344 b) The second part of the proof can be found in Branin (1963). It is shown there that the inverse of the
 345 tree incidence matrix is equal to the transpose of the node to datum path matrix of the tree, which can
 346 be determined, for instance, by use of basic graph algorithms (depth first search or breadth first search)
 347 or by a simple forward substitution process. \square

348 **Definition 1:**

349 Matrix $\mathbf{P} = -\mathbf{A}_{I,C} \mathbf{A}_{I,T}^{-1}$ is denoted as the internal tree matrix.

350 The positive direction of a superlink is determined by the direction of the internal co-tree chord. If the
 351 initial node of the internal co-tree chord link is a supernode then it will be the initial node of the
 352 superlink. In the opposite case where the last node of the internal co-tree chord is a supernode node
 353 then it will be the last node of the superlink. The directions of the branches of the internal tree are
 354 determined by the sign of the links in the internal tree matrix. A positive sign means that the direction
 355 of the link coincides with the direction of the superlink and vice versa.

356 Using Lemma 1, the unknown flows of the branches of the internal tree can be eliminated from the
 357 system of linear equations by solving the fourth row of the Global Linear System [GLS] (Eq. (12)) for
 358 $\mathbf{q}_{T,k+1}$:

$$359 \quad \mathbf{q}_{T,k+1} = \mathbf{P}^T \mathbf{q}_{C,k+1} - \mathbf{A}_{I,T}^{-T} \mathbf{Q}_I \quad (13)$$

360 Again, using Lemma 1, the unknown heads of the internal nodes can be eliminated from Eq. (12) by
 361 substituting $\mathbf{q}_{T,k+1}$ with use of Eq. (13) and solving the first row of Eq. (12) for $\mathbf{H}_{I,k+1}$:

$$362 \quad \mathbf{H}_{I,k+1} = \mathbf{A}_{I,T}^{-1} [\mathbf{h}_{T,k} - \mathbf{A}_{S,T} \mathbf{H}_{S,k+1} - \mathbf{A}_{R,T} \mathbf{H}_R] \quad (14)$$

363 where

$$364 \quad \mathbf{h}_{T,k} = [\mathbf{D}_{T,k} - \mathbf{F}_{T,k}] \mathbf{q}_{T,k} - \mathbf{D}_{T,k} [\mathbf{P}^T \mathbf{q}_{C,k+1} - \mathbf{A}_{I,T}^{-T} \mathbf{Q}_I]$$

365 Eq. (13) and Eq. (14) together can now be used for elimination of $\mathbf{q}_{T,k+1}$ and $\mathbf{H}_{I,k+1}$ from the second
 366 and third rows of Eq. (12). The resulting system of equations includes only the unknown heads of the
 367 supernodes $\mathbf{H}_{S,k+1}$ and the flows of the internal co-tree chords $\mathbf{q}_{C,k+1}$. With only a few algebraic
 368 manipulations we get:

$$369 \quad \begin{bmatrix} [\mathbf{D}_C + \mathbf{P} \mathbf{D}_T \mathbf{P}^T] & [\mathbf{A}_{S,C} + \mathbf{P} \mathbf{A}_{S,T}] \\ [\mathbf{A}_{S,C} + \mathbf{P} \mathbf{A}_{S,T}]^T & \mathbf{0} \end{bmatrix}_k \begin{bmatrix} \mathbf{q}_C \\ \mathbf{H}_S \end{bmatrix}_{k+1} = \begin{bmatrix} \bar{\mathbf{E}}_C \\ -\bar{\mathbf{Q}}_S \end{bmatrix}_k \quad (15)$$

370 with

$$371 \quad \bar{\mathbf{E}}_{C,k} = \mathbf{P}[\mathbf{D}_T - \mathbf{F}_T]_k \mathbf{q}_{T,k} + \mathbf{P}\mathbf{D}_{T,k}\mathbf{A}_{I,T}^{-T}\mathbf{Q}_I - \mathbf{P}\mathbf{A}_{R,T}\mathbf{H}_R + [\mathbf{D}_C - \mathbf{F}_C]_k \mathbf{q}_{C,k} - \mathbf{A}_{R,C}\mathbf{H}_R$$

$$372 \quad \bar{\mathbf{Q}}_{S,k} = -\mathbf{A}_{S,T}^T\mathbf{A}_{I,T}^{-T}\mathbf{Q}_I + \mathbf{Q}_S$$

373 **Network equations of the topological subgraph G_S**

374 In order to prove the analogy of the network equations of the graph G_S with the original equations the
375 topological incidence matrices of G_S are derived by linear transformations based on the internal tree
376 matrix given in Definition 1.

377 **Observation 1:**

378 a) Matrix $\mathbf{A}_{S,C} + \mathbf{P}\mathbf{A}_{S,T}$ is the incidence matrix of graph G_S consisting of superlinks (instead of the
379 original links) and supernodes (a subset of the original nodes): $\mathbf{A}_S = \mathbf{A}_{S,C} + \mathbf{P}\mathbf{A}_{S,T}$

380 b) Matrix $\mathbf{A}_{R,C} + \mathbf{P}\mathbf{A}_{R,T}$ is the incidence matrix of the fixed head nodes of graph G_S consisting of
381 superlinks (instead of the original links) and supernodes (a subset of the original fixed head nodes):

$$382 \quad \mathbf{A}_{S,R} = \mathbf{A}_{R,C} + \mathbf{P}\mathbf{A}_{R,T}.$$

383 c) Matrix $\mathbf{D}_{C,k} + \mathbf{P}\mathbf{D}_{T,k}\mathbf{P}^T$ is a diagonal matrix and corresponds to the derivatives of the hydraulic
384 head losses of the superlinks $\mathbf{D}_{S,k} = \mathbf{D}_{C,k} + \mathbf{P}\mathbf{D}_{T,k}\mathbf{P}^T$.

385 **Proof:**

386

387 a)

$$388 \quad \mathbf{A}_S = \mathbf{A}_{S,C} + \mathbf{P}\mathbf{A}_{S,T} = \mathbf{A}_{S,C} - \mathbf{A}_{I,C}\mathbf{A}_{I,T}^{-1}\mathbf{A}_{S,T}$$

389 Let us consider the rows of matrix $\mathbf{A}_{S,C}$ and distinguish between the following two cases when:

390 *1.) The internal tree together with internal co-tree consist of more than one link:*

391 For each internal tree together with its corresponding internal co-tree that consists of more than one
392 link, the corresponding row of the matrix $\mathbf{A}_{S,C}$ contains exactly one entry different from zero. This
393 entry belongs to the internal co-tree chord. The connection of the first supernode with the second
394 supernode is accomplished by $\mathbf{P}\mathbf{A}_{S,T}$. The rows of matrix \mathbf{P} correspond to superlinks, the columns
395 correspond to the original links (co-tree branches only). For each internal tree branch j that is part of
396 the superlink i the matrix entry P_{ij} is different from zero (-1 or +1). By definition, the mapping from

397 internal tree branches to superlinks is unique. The sign of $P_{i,j}$ indicates the direction of the branch
 398 relative to the superlink. Using the same argument that was used above for showing that matrix $\mathbf{A}_{S,C}$
 399 has exactly one element in row i that is different from zero it can be proven that the corresponding row
 400 in matrix $\mathbf{A}_{S,T}$ has also exactly one element different from zero and is therefore incident with the
 401 supernode of the internal tree. Pre-multiplication of the supernode - internal tree incidence matrix
 402 ($\mathbf{A}_{S,T}$) by the internal tree matrix (\mathbf{P}) select the root node of the internal tree as the second node of the
 403 superlink.

404 2.) *The superlink includes one link only:*

405 For each superlink containing only one link (the internal co-tree chord), the corresponding rows of
 406 matrix $\mathbf{A}_{S,C}$ have two elements in the same row that are different from zero. The internal tree matrix is
 407 the zero matrix. A simplification is not possible and the superlink incidence matrix and the link
 408 incidence matrix are identical.

409 b) The proof of part b) is analogous to that for part a).

410 c) The first term $\mathbf{D}_{C,k}$ includes the head loss derivatives of the internal co-tree chords. By calculation
 411 of the product of matrices $\mathbf{P}\mathbf{D}_{T,k}\mathbf{P}^T$, the head loss derivatives of the internal tree branches are summed
 412 up. The first multiplication by \mathbf{P} on the left replaces the -1 and +1 entries in the internal tree matrix by
 413 the head loss derivatives of the links. The second multiplication by the transpose of the internal tree
 414 matrix on the right of $\mathbf{D}_{T,k}$ computes the sum of the head loss derivatives for each internal tree. The
 415 result of the multiplication is again a diagonal matrix where each element on the main diagonal
 416 includes the sum of link head loss derivatives of the corresponding internal tree. It can be seen that the
 417 resulting matrix is diagonal due to the fact that the sets of internal tree branches are disjoint. That
 418 means that the multiplication delivers a value of zero, where the links are not in the same internal tree.

419 \square

420 With the results of Observation 1 then Eq. (15) can be rewritten as:

$$421 \begin{bmatrix} \mathbf{D}_S & \mathbf{A}_S \\ \mathbf{A}_S^T & \mathbf{0} \end{bmatrix}_k \begin{bmatrix} \mathbf{q}_C \\ \mathbf{H}_S \end{bmatrix}_{k+1} = \begin{bmatrix} \bar{\mathbf{E}}_C \\ -\bar{\mathbf{Q}}_S \end{bmatrix}_k \quad (16)$$

422 Matrix $\mathbf{D}_{S,k}$ is a diagonal matrix and invertible if $D_{S,i} > 0 \quad \forall i = 1, \dots, m_S$. Consequently, Eq. (16)

423 can be decomposed by using Schur's theorem analogously to the simplification of Eq. (5):

$$424 \quad \mathbf{q}_{C,k+1} = \mathbf{D}_{S,k}^{-1} \left[\mathbf{P}[\mathbf{D}_T - \mathbf{F}_T]_k \mathbf{q}_{T,k} + [\mathbf{D}_C - \mathbf{F}_C]_k \mathbf{q}_{C,k} + \mathbf{P} \mathbf{D}_{T,k} [\mathbf{A}_{I,T}^T]^{-1} \mathbf{Q}_I - \mathbf{A}_S \mathbf{H}_{S,k+1} - \mathbf{A}_{S,R} \mathbf{H}_R \right] \quad (17)$$

425 With $\mathbf{q}_{T,k} = \mathbf{P}^T \mathbf{q}_{C,k} - \mathbf{A}_{I,T}^{-T} \mathbf{Q}_I$ (Eq. (13)) it follows that:

$$426 \quad \mathbf{q}_{C,k+1} = \mathbf{q}_{C,k} - \mathbf{D}_{S,k}^{-1} [\mathbf{F}_{C,k} \mathbf{q}_{C,k} + \mathbf{P} \mathbf{F}_{T,k} \mathbf{P}^T \mathbf{q}_{C,k} - \mathbf{P} \mathbf{F}_{T,k} \mathbf{A}_{I,T}^{-T} \mathbf{Q}_I + \mathbf{A}_S \mathbf{H}_{S,k+1} + \mathbf{A}_{S,R} \mathbf{H}_R] \quad (18)$$

427 With the same arguments that were used for the elimination of \mathbf{q}_{k+1} in Eq. (5) now Eq. (18) can be

428 used for replacing the unknown flows $\mathbf{q}_{C,k+1}$ in the second row of Eq. (16):

$$429 \quad \mathbf{A}_S^T \mathbf{D}_{S,k}^{-1} \mathbf{A}_S \mathbf{H}_{S,k+1} = \bar{\mathbf{Q}}_S + \mathbf{A}_S^T \mathbf{q}_{C,k} - \mathbf{A}_S^T \mathbf{D}_{S,k}^{-1} [\mathbf{F}_{S,k} \mathbf{q}_{C,k} - \mathbf{P} \mathbf{F}_{T,k} \mathbf{A}_{I,T}^{-T} \mathbf{Q}_I + \mathbf{A}_{S,R} \mathbf{H}_R] \quad (19)$$

430 where $\mathbf{F}_{S,k} = \mathbf{F}_{C,k} + \mathbf{P} \mathbf{F}_{T,k} \mathbf{P}^T$ is analogous to Observation 1 c). By consideration of the fact that the

431 term $\mathbf{F}_{S,k} \mathbf{q}_{C,k} - \mathbf{P} \mathbf{F}_{T,k} \mathbf{A}_{I,T}^{-T} \mathbf{Q}_I$ is equal to the vector of head losses $\mathbf{h}_{S,k}$ of the superlinks at iteration k ,

432 Eq. (18) and Eq. (19) can be further simplified which finally leads to the main result of this paper. In

433 other words, the results of the solution of the reduced set of equations of the topological graph G_S

434 paper (Eq. (7) to Eq. (10)) are identical to the solution of the full set of equations for the core (Eq. (5)).

435 This completes the proof.

436 **Consideration of control devices**

437 Real water supply systems typically include, in addition to the pipes of the network, a number of

438 control devices and pumps for system operations. The devices are normally modelled as links and can

439 be subdivided into devices with given local headloss functions (TCV: throttle control valves) or

440 feedback control devices. The latter are used to control the flow and/or pressure by continuous

441 adjustment of the hydraulic resistance. Flow control is used either for allowing only unidirectional

442 flow (CHV) or maximum flow (FCV), whereas pressure control tries to maintain the downstream

443 (PRV) or upstream (PSV) head at a given set value. In EPANET control device models are based on a

444 set of heuristics that are described in the manual.

445 A simple way to tackle one-way devices in the GMPA approach is to set the initial and end nodes to

446 supernodes by definition. Then, the superlink consists of one link for the device only. The commonly

447 used heuristics for control devices can then be applied directly. However, the GMPA approach also

448 allows for consideration of flow control within a superlink. The only additional requirement is that the

449 control device link with the flow inequality condition is chosen as the internal tree chord. In this case
 450 the flow of the device link is identical with the superlink flow in the global system. Therefore, the
 451 linear inequality can be transferred to the global step as inequality condition for the superlink flow.
 452 If there is more than one device with inequality flow constraints included in the superlink then three
 453 cases have to be considered locally. 1.) There are contradictions between the constraints. There is no
 454 solution to the original system or the reduced system. 2.) The constraints are redundant. One device
 455 can be arbitrarily chosen. 3.) There are constraints that can never be active. Those that can be activated
 456 have to be identified. Note that the flows of any link can be always expressed by superposition of the
 457 internal tree chord flow and a constant local flow:

$$458 \quad \mathbf{q}_T = \mathbf{P}^T \mathbf{q}_C - \mathbf{A}_{I,T}^{-T} \mathbf{Q}_I$$

459 Therefore, the constraints (inequality or equality for gate valves) can be transferred from any link to
 460 the superlink flow.

461 Example: Assume that there is an inequality flow constraint representing a check valve in tree link j
 462 that belongs to superlink i , then: $\mathbf{q}_{T,i,j} \geq 0$, which is equivalent to $[\mathbf{P}^T]_{i,j} \mathbf{q}_{C,i} - [\mathbf{A}_{I,T}^{-T} \mathbf{Q}_I]_{i,j} \geq 0$.

463 $[\mathbf{P}^T]_{i,j}$ is +1 or -1 depending on the direction of flow in link j with respect to the direction of
 464 superlink i . The inequality condition for the superlink can now be written as $\mathbf{q}_{C,i} \geq [\mathbf{P}^T]_{i,j} [\mathbf{A}_{I,T}^{-T} \mathbf{Q}_I]_j$.

465 That means that only the right hand side of the inequality has changed As a consequence, even if the
 466 control link changes within the superlink (for example by closing different gate valves) there is no
 467 need to re-calculate the decomposition.

468

469 **EXAMPLE**

470 The system shown in Figure 1 is now used to illustrate the GMPA method. After forest – core –
 471 partitioning the core network (shown in Figure 4) consists of one reservoir (R) and eight demand
 472 nodes (a through h). There exist two nodes a and b that connect more than two pipes (degree > 2).

473 Therefore node a and node b are the supernodes of the network graph. The supernodes are connected
 474 by three superlinks. The pipe and node properties of the core are given in Table 1 and Table 2.

475 The first column in Table 1 refers to the pipe ID, L is the length in meters, D is the inner diameter of
 476 the pipe in millimeters, C denotes the Hazen-Williams coefficient and \mathbf{q}_0 is the initial guess of the

477 flows. The first column in Table 2 shows the identifier of the node and Q is the demand. A negative
478 sign means withdrawal. The last column shows the elevation of the node. With the parameters shown
479 in Table 1 and Table 2 including the internal tree flows as initial flow distribution q_0 , the flow iterates
480 of the new GMPA algorithm are as shown in Table 4. Note that the last four rows (for links 8, 9 10
481 and 1) refer to the internal tree chords representing the superlinks. The flows of the upper six internal
482 tree branches (links 2, 3, 4, 5, 6 and 7) are a linear function of the flows of the chords (Eq. (9)). The
483 reordered and partitioned incidence matrix of the original network graph is in compliance with Eq.
484 (11) and is:

485

486

487

$$\mathbf{A} = \begin{bmatrix} \mathbf{A}_{S,T} & \mathbf{A}_{I,T} \\ \mathbf{A}_{S,C} & \mathbf{A}_{I,C} \end{bmatrix} = \begin{array}{cccccccc|cc} \text{Nodes} & a & b & c & d & e & f & g & h & & \text{Links} \\ \hline & -1 & 0 & 1 & 0 & 0 & 0 & 0 & 0 & & 2 \\ & 0 & 0 & -1 & 1 & 0 & 0 & 0 & 0 & & 3 \\ & -1 & 0 & 0 & 0 & 1 & 0 & 0 & 0 & & 4 \\ & -1 & 0 & 0 & 0 & 0 & 1 & 0 & 0 & & 5 \\ & 0 & 0 & 0 & 0 & 0 & -1 & 1 & 0 & & 6 \\ & 0 & 0 & 0 & 0 & 0 & 0 & -1 & 1 & & 7 \\ \hline & 0 & 1 & 0 & 0 & -1 & 0 & 0 & 0 & & 8 \\ & 0 & 1 & 0 & -1 & 0 & 1 & 0 & 0 & & 9 \\ & 0 & 1 & 0 & 0 & 0 & 0 & 0 & -1 & & 10 \\ & 1 & 0 & 0 & 0 & 0 & 0 & 0 & 0 & & 1 \end{array}$$

488 The resulting topological matrices of graph G_S (taken from the 6 by 6 block of the upper right corner
489 of the \mathbf{A} matrix above and inverting the matrix analytically, Figure 5) are:

490

$$\mathbf{A}_{I,T}^{-1} = \begin{bmatrix} 1 & 0 & 0 & 0 & 0 & 0 \\ 1 & 1 & 0 & 0 & 0 & 0 \\ 0 & 0 & 1 & 0 & 0 & 0 \\ 0 & 0 & 0 & 1 & 0 & 0 \\ 0 & 0 & 0 & 1 & 1 & 0 \\ 0 & 0 & 0 & 1 & 1 & 1 \end{bmatrix}, \quad \mathbf{P} = -\mathbf{A}_{I,C} \mathbf{A}_{I,T}^{-1} = \begin{bmatrix} 0 & 0 & 1 & 0 & 0 & 0 \\ 1 & 1 & 0 & 0 & 0 & 0 \\ 0 & 0 & 0 & 1 & 1 & 1 \\ 0 & 0 & 0 & 0 & 0 & 0 \end{bmatrix}$$

491

$$\mathbf{A}_S = \mathbf{A}_{S,C} + \mathbf{P} \mathbf{A}_{S,T} = \begin{bmatrix} -1 & 1 \\ -1 & 1 \\ -1 & 1 \\ 1 & 0 \end{bmatrix}, \quad \mathbf{A}_{S,R} = \mathbf{A}_{R,C} + \mathbf{P} \mathbf{A}_{R,T} = \begin{bmatrix} 0 \\ 0 \\ 0 \\ -1 \end{bmatrix}$$

492

$$\bar{\mathbf{Q}}_S = -\mathbf{A}_{S,T}^T (\mathbf{A}_{I,T}^T)^{-1} \mathbf{Q}_I + \mathbf{Q}_S = \begin{bmatrix} Q_c + Q_d + Q_e + Q_f + Q_g + Q_h \\ 0 \end{bmatrix} + \begin{bmatrix} Q_a \\ Q_b \end{bmatrix} = \begin{bmatrix} -340 \\ -20 \end{bmatrix} \quad \left[\frac{m^3}{h} \right]$$

493 The demands of the supernodes and the internal nodes are included in $\bar{\mathbf{Q}}_S$. The reallocation of the
494 interior demand nodes is given by Eq. (6a) and depends on the choice of the internal tree chord. In the
495 example, the last link (connected to node b) of every superlink is chosen as internal tree chord. As a

496 consequence, the demands are all allocated to the upstream node, a. However, in general, the choice of
 497 another internal link as internal co-tree link can be useful, especially if control devices have to be
 498 considered. In such a case, by the application of Eq. (6a), parts of the interior node demands are
 499 allocated to the upstream supernode, and the other parts are allocated downstream.

500 The global/local factoring brings certain advantages when considering flow constraints associated with
 501 control devices For example, suppose that a check valve is placed on pipe 6 allowing flow only from
 502 node f to node g. Suppose also that a check valve is placed on pipe 7 allowing only flow from node h
 503 to node g. Pipe 6, for example, could be selected as the internal tree chord of the superlink that
 504 consists of link 5, 6, 7, 10. Then, the demand allocation is as follows:

$$505 \quad \bar{\mathbf{Q}}_S = -\mathbf{A}_{S,T}^T (\mathbf{A}_{I,T}^T)^{-1} \mathbf{Q}_I + \mathbf{Q}_S = \begin{bmatrix} Q_c + Q_d + Q_e + Q_f \\ Q_g + Q_h \end{bmatrix} + \begin{bmatrix} Q_a \\ Q_b \end{bmatrix} = \begin{bmatrix} -190 \\ -170 \end{bmatrix} \quad \begin{bmatrix} m^3 \\ h \end{bmatrix}$$

506 When considering the constraints of the two check valves it is sufficient to consider the local
 507 subsystem of the superlink. Furthermore, the flows of the superlink can be expressed as a linear
 508 function of the internal tree chord flow q_6 and the internal tree flows (which result from the interior
 509 node demands):

510 $q_5 = -Q_f + q_6$, $q_6 = q_6$, $q_7 = Q_g + q_6$, $q_{10} = Q_g + Q_h + q_6$. The two check valves are modelled by
 511 the following linear inequalities: $q_6 \geq 0$, $q_7 \leq 0 \Leftrightarrow Q_g + q_6 \leq 0 \Leftrightarrow q_6 \leq -Q_g$. It follows that
 512 $q_6 \in [0; -Q_g]$. Note that the demand (withdrawal at node g) has a negative sign. Therefore $-Q_g$ is
 513 positive. This means that the two check valves in the original network (and the local system of the
 514 superlink) have been modelled, in a preliminary step, by lower and upper bound constraints for the
 515 flow of the superlink. The global solution can be calculated by any existing technique which models
 516 control devices (see, for example Rossman (2000)). The flows are checked in case they exceed the
 517 upper or lower bounds. If they do, the flow in the superlink is set to the corresponding boundary value
 518 (in the example this is link 6 and its flow would be set to 0 for the lower bound, or $-Q_g$ for the upper
 519 bound.)

520 One advantage of the GMPA is that the local subsystems can be checked independently. Infeasible
 521 conditions can be detected before the iteration starts. In the example, such an infeasible condition
 522 occurs if the check valve of link 6 is replaced by an FCV and the direction of the CHV at link 7 allows

523 flow only from node g to node h . Thus, the conditions $q_6 \leq q_{Set}, q_7 \geq 0 \Leftrightarrow Q_g + q_6 \geq 0 \Leftrightarrow$
524 $q_6 \geq -Q_g$ apply. The constraint is now $-Q_g \leq q_6 \leq q_{Set}$. If the maximum flow q_{Set} for q_6 is
525 smaller than the withdrawal at node g there is no feasible solution in demand driven analysis. In the
526 state of the art package EPANET similar configurations often result in failure to converge or in
527 unrealistic results because of the singularity of the Jacobian matrix. GMPA analysis of the local
528 subsystems can detect infeasible sets of constraints *a priori*.

529 The reduction of the size of the problem by application of FCPA and GMPA is shown in Table 3. The
530 size of the final system dealt with in the GMPA is only 8% of the original network.

531

532 **CASE STUDIES**

533 Nine case-study networks, with between 900 and 64,000 pipes, and eight of which were considered in
534 Simpson et al. (2014), illustrate the significant reduction achieved by GMPA in the size of the
535 nonlinear problem that must be solved. Table 5 shows, for these networks, the basic dimensions of the
536 nonlinear part of the problem before the forest-core partitioning, after the forest-core partitioning, and
537 after the graph matrix partitioning step of the GMPA: the resulting problems have dimension between
538 5% and 55%, with a mean 27% (a 73% reduction in dimension), of the core dimension that results
539 from application of the forest-core partitioning.

540 The data for case study networks N_1 , N_3 , N_4 and N_7 , which are slight modifications of networks in the
541 public domain, are available as Supplemental Data Files. The other four networks considered in this
542 paper are not available because of security concerns.

543

544 **CONCLUSIONS**

545 The Graph Matrix Partitioning Algorithm (GMPA) developed in this paper, when applied to networks
546 that have many core pipes in series, can save a significant computational effort by reducing the size of
547 the problem for the most time consuming part of the calculation. The FCPA step, applied before the
548 main GMPA step, separates the forest from the core, thereby reducing the dimension of the non-linear
549 part of the problem when a forest is present. The GMPA step, the separation or partitioning of the
550 topological subgraph from the core, further separates linear and nonlinear parts of the problem and

551 further reduces the dimension of the non-linear part of the problem when there are pipes in series
552 within the core. These two steps, which separate out the linear and non-linear parts of the problem and
553 then deal with them using appropriate linear and non-linear methods, save much time that is otherwise
554 wasted applying non-linear techniques to problems which have significant linear components.

555

556 The permuted system is decomposed into a global solution for the maximal topological subgraph
557 G_S and a local solution for the internal trees with nodes of degree two. The iterative solution of the
558 smaller system of equations of G_S in combination with the linear local steps gives identical results to
559 those obtained from the standard solution to the full network system. *There are no approximations.*

560 The equivalence of the GMPA and the original set of equations has been proven.

561 Real world applications have shown reductions from 5,000 unknown in the system of equations to 150
562 or even 230,000 unknowns to 10,000 unknowns. On average, the number of unknowns in the
563 nonlinear (core) part of the problem for the systems tested was less than 20% of the original size. The
564 case studies reported in Table 5 show that GPMA achieves a reduction to between 5% and 55% of the
565 core dimension that results from application of the FCPA. In the GMPA method, all the important
566 properties of the system matrix of the original system are retained (sparse, symmetric, Stieltjes matrix)
567 and the same efficient factorization methods can be applied to the reduced system.

568 Last, but not least, the linear mapping between topological subgraph and original graph can be used
569 for other applications. The aggregation methods for simplification of large networks can be replaced
570 by an adaptive modelling based on the topological subgraph. As a consequence, the process of
571 updating existing models from GIS is much easier since the one to one mapping between GIS features
572 and network model features is always valid and not lost by aggregation.

573

574 The focus of this paper is on the derivation of, and the theoretical basis for, the GMPA method. The
575 efficiency of a production implementation of method depends on many factors, including, for
576 example, the architecture of the computing platform and the coding language. The global and local
577 steps can be handled separately: by separate program codes or even on separate architectures. In the
578 case where a coarse grid approximation to the solution is all that is required, the user can simply solve

579 the global step: the method can be used in the same way as common aggregation techniques that
580 calculate an approximate solution Where the complete solution is required the local and global steps of
581 the GMPA can be implemented by different codes or on even on different architectures. Where
582 separate architectures are used for the global and local steps the data exchange required is minimal, a
583 significant advantage of the GMPA. Thus, an existing nonlinear solver code can be used by adding to
584 it a separate package to handle the local step in the algorithm. The GMPA is also well suited to handle
585 the inclusion of control devices and parts of the method are well suited to parallelization.

586 Further research in the application of GMPA to the solution of pressure dependent models would
587 be a useful contribution to the field. Another contribution to the field would be a comprehensive study
588 of just how large would be the time savings available by use of the GMPA. Study of these issues is
589 well beyond the scope of this paper.

590

591 **ACKNOWLEDGEMENTS**

592

593 The work presented in this paper has been partly developed as part of the research project SMaRT-
594 Online^{WDN} (Code 13N12178) that is funded by the German Federal Ministry of Education and
595 Research (BMBF) and the French National Research Agency (ANR).

596

597 **APPENDIX A: Calculation of permutation matrices**

598 The system in Eq. (12), in which the matrix, \mathbf{A} , on the left has its rows and columns permuted in the
599 required order, as shown in Eq. (11), and the matrix, \mathbf{D} , is diagonal, can be obtained from the original
600 system (Eq. (5)**Error! Reference source not found.**) as follows. Suppose the original system is

$$601 \begin{bmatrix} \hat{\mathbf{D}} & \hat{\mathbf{A}} \\ \hat{\mathbf{A}}^T & \mathbf{0} \end{bmatrix} \begin{bmatrix} \Delta \hat{\mathbf{Q}} \\ \Delta \hat{\mathbf{H}} \end{bmatrix} = \begin{bmatrix} d \hat{\mathbf{E}} \\ d \hat{\mathbf{Q}} \end{bmatrix} \quad (\text{A.1})$$

602 and that the $m \times n$ incidence matrix $\hat{\mathbf{A}}$ (m : total number of links, n : total number of nodes) has its
603 rows and columns in an order different from that which is required. Suppose $\mathbf{R} \in \mathbb{R}^{m \times m}$ and $\mathbf{S} \in$
604 $\mathbb{R}^{n \times n}$ are (orthogonal) permutation matrices which are such that $\mathbf{R}\hat{\mathbf{A}}\mathbf{S}$ has its rows and columns in the
605 required order. Then, multiplying (A.1) on the left by

606

$$\begin{bmatrix} \mathbf{R} & \\ & \mathbf{S}^T \end{bmatrix}$$

607 and inserting the product

608

$$\begin{bmatrix} \mathbf{R}^T & \\ & \mathbf{S} \end{bmatrix} \begin{bmatrix} \mathbf{R} & \\ & \mathbf{S}^T \end{bmatrix} = \mathbf{I}$$

609 between the matrix and vector on the left gives

$$\begin{bmatrix} \mathbf{R} & \\ & \mathbf{S}^T \end{bmatrix} \begin{bmatrix} \hat{\mathbf{D}} & \hat{\mathbf{A}} \\ \hat{\mathbf{A}}^T & \mathbf{0} \end{bmatrix} \begin{bmatrix} \mathbf{R}^T & \\ & \mathbf{S} \end{bmatrix} \begin{bmatrix} \mathbf{R} & \\ & \mathbf{S}^T \end{bmatrix} \begin{bmatrix} \Delta \hat{\mathbf{q}} \\ \Delta \hat{\mathbf{H}} \end{bmatrix} = \begin{bmatrix} \mathbf{R} & \\ & \mathbf{S}^T \end{bmatrix} \begin{bmatrix} d\hat{\mathbf{E}} \\ d\hat{\mathbf{Q}} \end{bmatrix}, \quad (\text{A.2})$$

611 Denoting

$$612 \quad \mathbf{A} = \mathbf{R}\hat{\mathbf{A}}\mathbf{S}, \mathbf{D} = \mathbf{R}\hat{\mathbf{D}}\mathbf{R}^T, \Delta \mathbf{q} = \mathbf{R}\Delta \hat{\mathbf{q}}, \Delta \mathbf{H} = \mathbf{S}^T \Delta \hat{\mathbf{H}}, \mathbf{a}_1 = \mathbf{R}\hat{\mathbf{a}}_1, \mathbf{a}_2 = \mathbf{S}^T \hat{\mathbf{a}}_2$$

613 means that (A.1) can be rewritten as

$$614 \quad \begin{bmatrix} \mathbf{D} & \mathbf{A} \\ \mathbf{A}^T & \mathbf{0} \end{bmatrix} \begin{bmatrix} \Delta \mathbf{q} \\ \Delta \mathbf{H} \end{bmatrix} = \begin{bmatrix} d\mathbf{E} \\ d\mathbf{Q} \end{bmatrix}, \quad (\text{A.3})$$

615 the system in Eq. (12) with consideration of Eq. (11) in which \mathbf{A} has its rows and columns permuted as616 required. By multiplication of the incidence matrix with the matrix \mathbf{S} the columns that belong to617 supernodes are separated from the columns that belong to inner nodes. Matrix \mathbf{S} can be easily618 determined by traversing the network nodes and selecting first all the n_s nodes that have degree > 2

619 followed by the rest of the nodes.

620 Multiplication by matrix \mathbf{R} separates the internal tree branches of the superlinks from the internal co-

621 tree chords.

622

623 **REFERENCES**

- 624 Branin, F. Jr. (1963): "The Inverse of the Incidence Matrix of a Tree and the Formulation of the
625 Algebraic-First-Order Differential Equations of an RLC Network", *IEEE Transac. on Circuit Theory*,
626 Vol. 10, No. 4, pp. 543 – 544. [doi: 10.1109/TCT.1963.1082204](https://doi.org/10.1109/TCT.1963.1082204)
- 627 Birkhoff, G. and Diaz, J.-B. (1956): "Non-linear network problems", *Quarterly of Applied*
628 *Mathematics*, Vol. 13, No. 4, pp. 431 – 443.
- 629 Birkhoff, G. (1962): "A variational principle for nonlinear networks", *Quarterly of Applied*
630 *Mathematics*, Vol. 21, No. 2, pp. 160 – 162.
- 631 Carpentier, P. and Cohen, G. (1993): "Applied Mathematics in Water Supply Network Management",
632 *Automatica*, Vol. 29, No. 5, pp. 1215 – 1250. [doi: 10.1016/0005-1098\(93\)90048-X](https://doi.org/10.1016/0005-1098(93)90048-X)
- 633 Cherry, C. (1951): "Some general theorems for non-linear systems possessing reactance," *The*
634 *Philosophical Magazine*, Vol. 42, No. 7, pp. 1161 – 1177.
- 635 Collins, M.; Cooper, L.; Helgarson, R.; Kennington, J. L. and LeBlanc, L. (1978): "Solving the pipe
636 network analysis problem using optimization techniques", *Management Science*, Vol. 24, No. 7, pp.
637 747-760. [doi: 10.1287/mnsc.24.7.747](https://doi.org/10.1287/mnsc.24.7.747)
- 638 Cross, H. (1936): "Analysis of flow in networks of conduits or conductors", *Bulletin No. 286*,
639 Engineering Experiment Station, Univ. of Illinois, Urbana, IL.
- 640 Deuerlein, J. W. (2008): "Decomposition model of a general water supply network graph", *Journal of*
641 *Hydraulic Engineering*, Vol. 134, No. 6, pp. 822 - 832. [doi: 0.1061/\(ASCE\)0733-9429\(2008\)134:6\(822\)](https://doi.org/0.1061/(ASCE)0733-9429(2008)134:6(822))
- 642 Deuerlein, J. W.; Simpson, A. R. and Dempe, S. (2009): "Modeling the Behavior of Flow Regulating
643 Devices in Water Distribution Systems Using Constrained Nonlinear Programming", *Journal of*
644 *Hydraulic Engineering*, Vol. 135, No. 11, pp. 970-982. [doi: 0.1061/\(ASCE\)HY.1943-7900.0000108](https://doi.org/0.1061/(ASCE)HY.1943-7900.0000108)
- 645 Diestel, R. (2010): "Graph theory," 4th Edition, GTM 173, Springer Verlag, Heidelberg, New York.
- 646 Epp, R. and Fowler, A. (1970): "Efficient code for steady-state flows in networks", *Journal of the*
647 *Hydraulics Division*, Vol. 96, No. HY1, pp. 43-56.

648 Elhay, S., Simpson, A., Deuerlein, J., Alexander, B., and Schilders, W. (2014). "Reformulated Co-
649 Tree Flows Method Competitive with the Global Gradient Algorithm for Solving Water Distribution
650 System Equations." *J. Water Resour. Plann. Manage.*, 140(12), 04014040.

651 Giustolisi, O. (2010): "Considering Actual Pipe Connections in Water Distribution Network
652 Analysis", *Journal of Hydraulic Engineering*, Vol. 136, No. 11, 2010, pp. 889 – 900. doi:
653 [10.1061/\(ASCE\)HY.1943-7900.0000266](https://doi.org/10.1061/(ASCE)HY.1943-7900.0000266)

654 Giustolisi, O.; Laucelli, D.; Berardi, L. and Savic, D. (2012) "Computationally Efficient Modeling
655 Method for Large Water Network Analysis", *Journal of Hydraulic Engineering*, Vol. 138, No. 4, pp.
656 313 – 326. doi: [0.1061/\(ASCE\)HY.1943-7900.0000517](https://doi.org/10.1061/(ASCE)HY.1943-7900.0000517)

657 Gupta, R. and Prasad, T. D. (2000): "Extended use of linear graph theory for analysis of pipe
658 networks", *Journal of Hydraulic Engineering*, Vol. 126, No. 1, pp. 56–62. doi: [10.1061/\(ASCE\)0733-
659 9429\(2000\)126:1\(56\)](https://doi.org/10.1061/(ASCE)0733-9429(2000)126:1(56))

660 Kesavan, H. K.; Chandrashekar, M. (1972): "Graph-theoretic models for pipe network analysis",
661 *Journal of the Hydraulics Division*, Vol. 98, No. HY2, 1972, pp. 345–363.

662 Millar, W. (1951): "Some general theorems for non-linear systems possessing resistance", *The
663 Philosophical Magazine*, Vol. 42, No. 7, pp. 1150 – 1160.

664 Nielsen, H. B. (1989): "Methods for analyzing pipe networks", *Journal of Hydraulic Engineering*,
665 Vol. 115, No. 2, 1989, pp. 139-157. doi: [10.1061/\(ASCE\)0733-9429\(1989\)115:2\(139\)](https://doi.org/10.1061/(ASCE)0733-9429(1989)115:2(139))

666 Piller, O. (1995). "Modeling the behavior of a network - Hydraulic analysis and sampling procedures
667 for parameter estimation," Applied Mathematics thesis from the University of Bordeaux, 288 pages,
668 Talence, France.

669 Rossman, L. A. (2000): "EPANET 2 Users manual", EPA/600/R-00/057, Environmental Protection
670 Agency, Cincinnati, Ohio, USA.

671 Schilders, W. (2009): "Solution of indefinite linear systems using an LQ decomposition for the linear
672 constraints", *Linear Algebra and its Applications*, Vol. 431, No. 3 – 4, pp. 381 – 395. doi:
673 [10.1016/j.laa.2009.02.036](https://doi.org/10.1016/j.laa.2009.02.036)

674 Simpson, A. R. and Elhay, S. (2011): "The Jacobian for solving water distribution system equations
675 with the Darcy-Weisbach head loss model," *Journal of Hydraulic Engineering* Vol. 137, No. 6, pp.
676 696-700. [doi: 10.1061/\(ASCE\)HY.1943-7900.0000341](https://doi.org/10.1061/(ASCE)HY.1943-7900.0000341)

677 Simpson, A. R., Elhay, S., and Alexander, B. (2014). "A Forest-Core Partitioning Algorithm for
678 Speeding up the Analysis of Water Distribution Systems." *J. Water Resour. Plann. Manage.*, 140(4),
679 435–443. [doi: 10.1061/\(ASCE\)WR.1943-5452.0000336](https://doi.org/10.1061/(ASCE)WR.1943-5452.0000336)

680 Todini, E. and Rossman, L. A. (2013): "Unified Framework for Deriving Simultaneous Equation
681 Algorithms for Water Distribution Networks," *Journal of Hydraulic Engineering*, Vol. 139, No. 5, pp.
682 511 – 526. [doi: 10.1061/\(ASCE\)HY.1943-7900.0000703](https://doi.org/10.1061/(ASCE)HY.1943-7900.0000703)

683 Todini, E. and Pilati, S. (1988): "A gradient algorithm for the analysis of pipe networks," *Computer*
684 *Applications in Water Supply*, Research Studies Press, Letchworth, Hertfordshire, UK.

Table 1: Pipe properties of core of example network (after application of the FCPA)

Pipes	L [m]	D [mm]	C [-]	q_0 [m ³ /h]
1	1000	300	100	0
2	1000	200	100	70
3	1500	150	100	40
4	1200	200	100	50
5	800	200	100	210
6	800	150	100	150
7	800	150	100	80
8	1200	100	100	0
9	1000	100	100	0
10	800	100	100	0

Table 2: Node properties of core of example network (after application of the FCPA)

Nodes	Q[m ³ /h]	H ₀ [m]
a	-10	1
b	-20	1
c	-30	1
d	-40	1
e	-50	1
f	-60	1
g	-70	1
h	-80	1
R	360	150

Table 3: Reduction in size of the nonlinear problem by application of the GMPA method

Step	number of nodes	number of links	reduction of number of nodes [%]
Original network Fig. 1	38	39	-
After forest-core partitioning. Fig. 2	9	10	76
After topological partitioning (GMPA). Fig 3	3	4	92

Table 4: Flow iterates of the GMPA (m³/s)

k =	0	1	2	3	4	5
2	0.01944	0.01859	0.02382	0.02508	0.02519	0.02519
3	0.01111	0.01026	0.01548	0.01675	0.01685	0.01685
4	0.01389	0.03868	0.02632	0.02286	0.02251	0.02250
5	0.05833	0.03995	0.04709	0.04928	0.04953	0.04953
6	0.04167	0.02328	0.03042	0.03262	0.03286	0.03286
7	0.02222	0.00384	0.01098	0.01317	0.01342	0.01342
8	0.00000	0.02479	0.01243	0.00897	0.00862	0.00861
9	0.00000	-0.00086	0.00437	0.00563	0.00574	0.00574
10	0.00000	-0.01838	-0.01124	-0.00905	-0.00880	-0.00880
1	0.00000	0.10000	0.10000	0.10000	0.10000	0.10000

Table 5: Network dimensions before forest partitioning (m pipes, n nodes), after forest partitioning (\tilde{m} pipes, \tilde{n} nodes), and after graph matrix partitioning (\hat{m} pipes, \hat{n} nodes) together with partitioned dimensions as percentages

DI	m	n	\tilde{m}	\tilde{n}	\hat{m}	\hat{n}	$\frac{\tilde{n}}{n}\%$	$\frac{\hat{n}}{\tilde{n}}\%$	$\frac{\hat{n}}{n}\%$
N1	934	848	573	487	246	160	57	33	19
N2	1118	1039	797	718	235	156	69	22	15
N3	1976	1770	1153	947	547	341	54	36	19
N4	2465	1890	2036	1461	1379	804	77	55	43
N5	2508	2443	1806	1741	187	122	71	7	5
N6	8584	8392	6734	6542	542	350	78	5	4
N7	14830	12523	11898	9591	6405	4098	77	43	33
N8	19647	17971	15233	13557	4878	3202	75	24	18
N9	63829	59157	51845	47173	14228	9556	79	20	16
	Means						71%	27%	19%

.

Captions of Figures:

Figure 1: Example network graph.

Figure 2: The core of the example network graph (after forest-core partitioning)

Figure 3: Links and nodes of a superlink.

Figure 4: Labelled core of the example network graph.

Figure 5: Topological minor (topological subgraph) of the core of the example

Figure 1
[Click here to download Figure: Fig1.pdf](#)

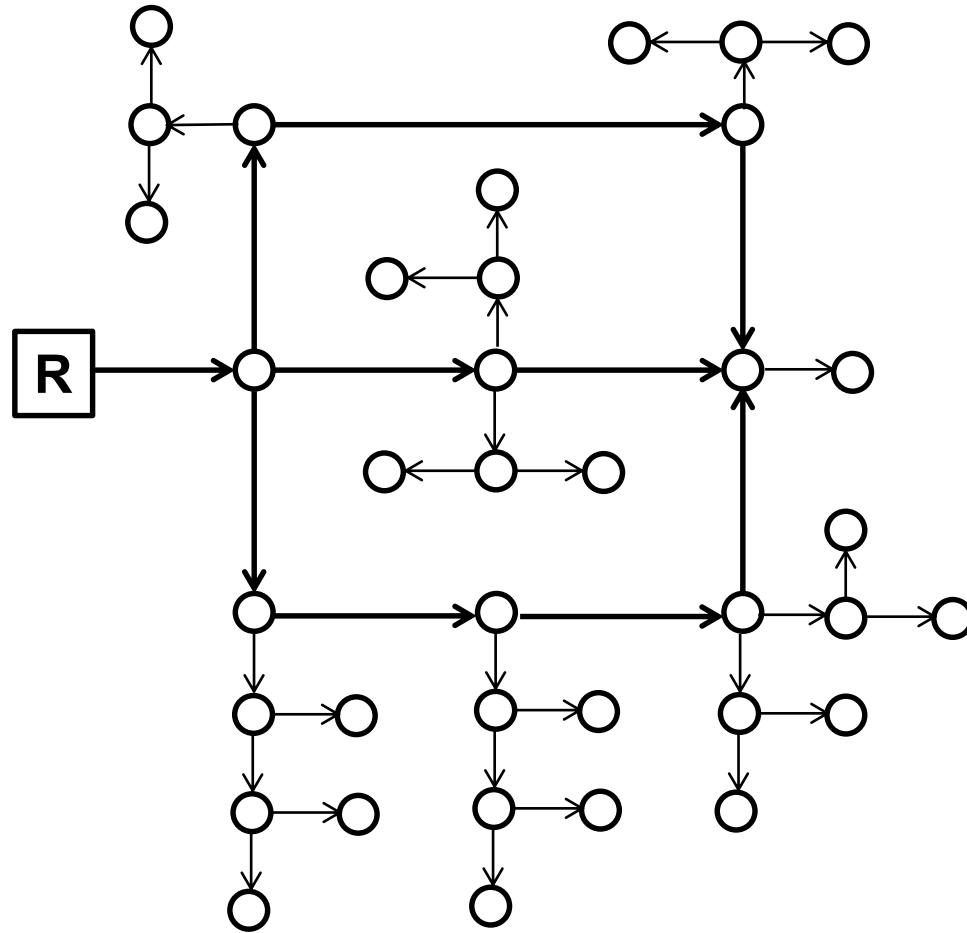


Figure 2

[Click here to download Figure: Fig2.pdf](#)

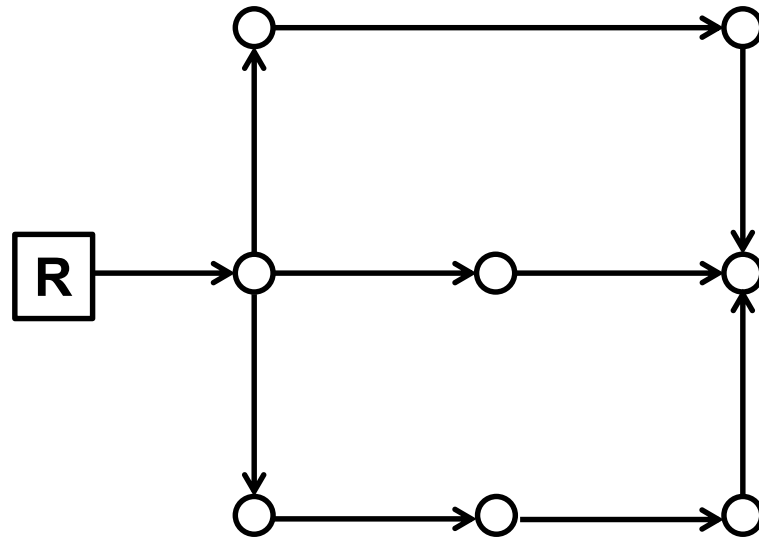
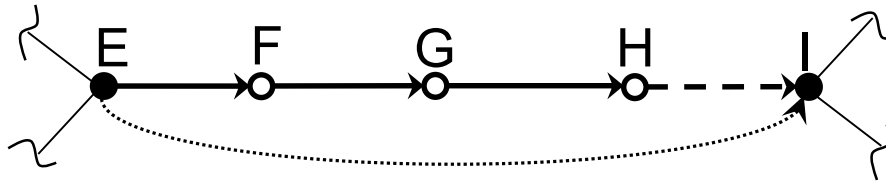


Figure 3

[Click here to download Figure: Fig3.pdf](#)



- 1.) ● supernodes (E, I)
- 2.) ○ internal tree nodes (F, G, H)
- 3.) → internal tree branches (EF, FG, GH) (E to H is the internal tree)
- 4.) - → internal co-tree chord (HI)
- 5.) → superlink (EI)

Figure 4
[Click here to download Figure: Fig4.pdf](#)

